

# Ultimate photo-induced Kerr rotation achieved in semiconductor microcavities

R. V. Cherbunin, A. V. Mikhailov, and N. E. Kopteva  
*St Petersburg State University, 198504 Russia*

M. Vladimirova  
*Laboratoire Charles Coulomb, University Montpellier, France*

K. V. Kavokin  
*St Petersburg State University, 198504 Russia and  
Ioffe Physical-Technical Institute, St Petersburg, Russia*

P. G. Lagoudakis  
*Department of Physics & Astronomy, University of Southampton, Southampton SO17 1BJ, United Kingdom*

A. V. Kavokin  
*St Petersburg State University, 198504 Russia and  
Department of Physics & Astronomy, University of Southampton, Southampton SO17 1BJ, United Kingdom*  
(Dated: March 1, 2019)

Giant Kerr rotation and ellipticity are observed and investigated in an asymmetric planar microcavity with a quantum well in the active region. Rotation angle of the polarization plane as well as ellipticity were determined from time- and frequency resolved measurements of the Stokes vector components of reflected light. It was found that at negative detuning of the cavity mode with respect to the heavy exciton transition, the splitting of lower polariton branch under circularly polarized pump can exceed its linewidth. This fact gives a possibility to observe the Kerr rotation angle and ellipticity, close to their extremes. A theoretical analysis shows that the decisive role in reaching extreme polarization rotation angles is played not by the quality factor of the cavity, but by the structure asymmetry, which provides optical impedance matching at small negative detunings of the photon mode with respect to the exciton resonance. The possibility of application of the studied effect for fast optical switching is discussed.

PACS numbers: 71.36.+c, 42.65.-k

Last decades are marked with widespread use of photoinduced Kerr and Faraday rotation for studying of spin-related phenomena in semiconductor nanostructures [2]. The success of this approach is due to the fact that resonant light-matter coupling gives a possibility to obtain easily detectable signals, of the order of mrad, even from nanometer-sized objects. Even stronger Faraday/Kerr rotation can be obtained by placing a nano-object, like a quantum well or a layer of quantum dots, inside a planar microcavity [8, 9].

This way, the rotation signal can be enhanced by several orders of magnitude, thanks to high optical quality factors of semiconductor microcavities [5, 7]. In some cases, the enhancement is strong enough to devise new types of experiments. In particular, in Ref. [1] Kerr rotation by a single electron spin was observed, and in Faraday rotation by polarized nuclear spins in in Ref.[6] Faraday rotation by polarized nuclear spins in a semiconductor was realized and investigated. As spin noise and Kerr rotation have the same origin, placing the source of the spin noise into a microcavity also results in its amplification [12].

The possibility to rotate, with optical pumping, the polarization plane of a probe beam by 90 degrees or

more would be very attractive since it could provide a base for development of superfast all-optical light modulators. To the best of our knowledge, this was not so far demonstrated. Seemingly, strong-coupling quantum-well microcavities are excellent candidates for realization of large rotation angles, because of efficient coupling of the electromagnetic field with material resonances (excitons). However, experimentally observed polarization rotation angles in structures with microcavities do not exceed several degrees [4], though its theoretical limit equals  $2\pi$ [8].

The enhancement of Kerr and Faraday rotations in the Fabry-Pérot resonator is due to an abrupt change of the phase of reflected or transmitted light when crossing the frequency of the photon mode. This effect results from interference of light reflected by mirrors forming the planar cavity, and does not depend on the presence of an active media inside the cavity. It is because of this effect that Fabry-Pérot etalons are applied not only as spectral filters of the light intensity, but also for producing a sharp dependence of the phase of reflected light: for example, for the compensation of dispersion in pulsed lasers or in systems of active stabilization of frequency [3]. However, in semiconductor quantum well microcavities this sharp

and monotonous frequency dependence of the reflection phase can be realized only at negative detuning of the photonic mode from the exciton resonance, where losses in the cavity are small. For this reason, in the spectral region near the exciton resonance, where the Faraday/Kerr signal from the quantum well would be the strongest, the cavity may give no advantage at all. The enhancement of the rotation signal occurs only at large enough negative detuning, where the exciton contribution into the dielectric function and, as a consequence, the exciton-induced gyrotropy may be already small.

In the following, we will concentrate on polarization rotation in the reflection geometry (magneto-optical or photoinduced Kerr effect). The spectral behavior of the phase of the light wave reflected from a Fabry-Pérot resonator with highly reflecting back mirror (which is typically the case for semiconductor microcavities) is known to be determined by the way in which the reflected wave is formed. Generally, it is contributed by the wave reflected from the front mirror and by the wave leaking from the cavity, besides their relative weights depend on the relationship between losses in the cavity and the front mirror reflectivity. At very low resonator losses, a standing wave of large amplitude forms inside the cavity, giving rise to an intense leakage wave. At the resonance frequency, its amplitude exceeds the amplitude of directly reflected wave by factor 2, while their phases are opposite. In this case the spectral dependence of the reflection phase is monotonous, with the phase changing from 0 to  $2\pi$  in crossing the resonance. If absorption in the cavity is strong, then the amplitude of the standing wave is small, the leakage wave is weak, and the reflected wave is formed mainly by the front mirror. In this case, the role of cavity in light reflection from the structure is insignificant. With respect to the phase, this means that it does not change by  $2\pi$  when passing the resonance, and the spectrum of reflection phase has the shape of the derivative of Lorentz contour with a small magnitude. In between these two extreme cases, there exists certain level of losses at which the leakage wave and directly reflected wave at the resonance have equal amplitudes and opposite phases. In this case reflection at the resonance frequency completely disappears (sometimes this regime is called the regime of impedance matching, because all the incident power is absorbed in the cavity).

In spite of the obvious importance of this effect, it was, to the best of our knowledge, rarely taken into consideration when working with semiconductor microcavities. In Ref. [11], a principle of electric control over the phase of reflected light was proposed, based on energy level shifts in double-quantum-well structure placed in a microcavity that resulted in modulation of losses in the cavity. In the work [14] Kerr rotation changed its spectral shape under heating of the microcavity structure from 4 to 150 K from a single peak at low temperature to a bipolar structure, resembling the Lorentz derivative, at about

100 K. This effect was partly explained by variation of light absorption by density-of-state tails in mirrors, which could change relative contributions of directly reflected and leakage waves. Finally, in our work [12] peculiarities of the spin-noise optical spectra were observed and analysed near the impedance matching point of a microcavity.

In this Letter, we experimentally and theoretically investigate the behavior of photoinduced Kerr effect in a semiconductor microcavity near the impedance matching point. In particular, we find out, what rotation angles can be reached, and what are the microscopic mechanisms that are responsible for enhanced gyrotropy of such a structure under optical pumping.

We used a microcavity structure grown by molecular beam epitaxy on a GaAs substrate. The structure comprised a  $1\lambda$ -cavity with a 20-nm quantum well (QW) in the center, formed by two planar Bragg mirrors. Front and rear Bragg mirrors consisted, of 15 and 25 pair of quarter-wavelength layers of AlAs/Al<sub>0.1</sub>Ga<sub>0.9</sub>As, respectively. The cavity width was graded along the structure plane, giving a possibility to perform measurements at different detunings of the photon mode from the exciton resonance in the QW. The structure design has been described in more detail in Ref. [10, 13].

This structure was investigated in the backscattering geometry using the time-resolved pump-probe method. The gyrotropy in the active layer was created by circularly polarized pulses of a mode-locked Ti:Sapphire laser by pumping into the upper polariton branch. The laser was operated in the femtosecond regime. Spectrally narrow pump pulses were cut from the broad spectrum of the femtosecond pulse by an acousto-optic filter, which allowed us to adjust the time-integrated power of the pump beam in the range 0-20 mW. Because the reflection coefficient on the upper polariton branch strongly depends on detuning, in the following we use optical power, absorbed in the sample, instead of the incident power, assuming that all of the power transmitted through the front mirror is absorbed in the QW. Probe pulses were left spectrally wide, so that they covered all the studied resonances. The probe beam was linearly polarized in the vertical plane and had the time-integrated power of 0.1 mW. The time delay between pump and probe pulses was provided by a 1m motorized optical delay line.

Two methods were used for measuring the polarization of reflected probe light. An optical bridge with balanced photodiodes was used when the photoinduced rotation angles were within  $\pm\pi/4$ . In order to measure rotation angles outside this range, as well as for distinguishing among Kerr rotation, induced ellipticity and depolarization, a different method was used. In this case the Stokes parameters of the reflected probe beam:

$$S_i = \frac{I_\mu - I_\nu}{I_\mu + I_\nu},$$

where  $I_{\mu,\nu}$  is the intensity of light components polarized along horizontal ( $\mu = H$ ) and vertical ( $\nu = V$ ) axes, diagonal (rotated by  $\pi/4$ ) axes:  $\mu = D$ ,  $\nu = A$ , and of circularly polarized components:  $\mu = \sigma+$ ,  $\nu = \sigma-$ , were measured using an ellipsometer. The ellipsometer consisted of two phase plated (with half-wave and quarter-wave retardation) and a linear polarizer, installed one after another in front of the entrance slit of a 0.5-m spectrometer equipped with a CCD camera. For each delay between pump and probe, spectra of the reflected probe pulses were recorded in six different polarizations: vertical, horizontal, diagonal, anti-diagonal, right circular and left circular, which then were used to calculate spectral dependences of the Stokes parameters.

To avoid the influence of intrinsic anisotropy of the sample, it was oriented so that the crystallographic axis (110) was inside the polarization plane of the incident probe beam. The sample was placed in a closed-cycle optical cryostat at 4.2K. Pump and probe beams were focused into a 50  $\mu\text{m}$  spot on the sample surface using a lens with 100 mm focal length.

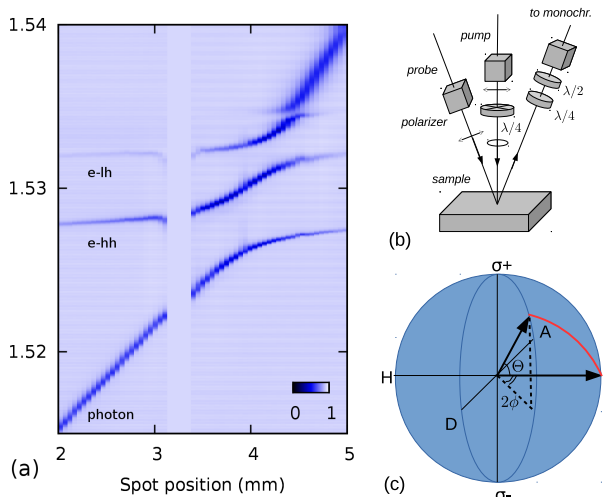


Figure 1. (Color online) (a) Reflection spectrum of the structure as a function of position in the structure plane. (b) Polarimetric part of the experimental setup. (c) Kerr rotation angle  $\phi_k$  and ellipticity angle  $\Theta$  on Poincaré sphere.

In order to characterize the studied structure, we measured reflectivity spectra near the anticrossing of the cavity mode with exciton resonances in the QW for different detunings. Figure 1(a) shows the reflectivity as a function of photon energy and position on the sample surface ( $x$ ). The energy of cavity mode shifts approximately linearly with the coordinate  $x$ . For each position, three dips are observed, corresponding to the cavity photon mode (MC-mode), heavy (X) and light (LX) exciton. At the point  $x \simeq 3.7$  mm an anticrossing of the cavity mode with a heavy-hole exciton is observed, while at  $x \simeq 4.0$  mm it anti-crosses with the light-hole exciton. Further,

at  $x \simeq 4.5$  mm MC mode anti-crosses with yet another resonance, which is attributed to the exciton formed by the ground-state heavy hole and an electron on the second level of size quantization in the QW.

As seen from this plot, the strong coupling regime is realized in the studied microcavity structure, besides the splitting of polariton branches is approximately 10 times larger than their widths. Because of moderate quality factor of our microcavity, the width of the cavity mode far from the anti-crossing point is even larger than the width of heavy exciton resonance (0.3 meV and 0.15 meV, respectively). Above the anti-crossing point with the upper exciton level, the MC mode width becomes several times larger due to inter-band absorption in the QW and increased losses in mirrors.

Our measurements of Kerr rotation under weak optical pumping  $P \simeq 1$  mW have shown that the largest rotation signal is observed at small negative detuning of the MC mode  $\Delta = -3.. -5$  meV. The excitation spectrum of Kerr rotation detected on the MC mode has several peaks of different polarity, the most intense of which corresponds to the heavy exciton resonance. Irrespective of detuning, the kinetics of Kerr rotation consists of a zero-delay peak with the width of the order of 10 ps, followed by a biexponential decay. The first exponential has the time decrement of the order of 500 ps, determined by spin relaxation of photoexcited excitons. The second

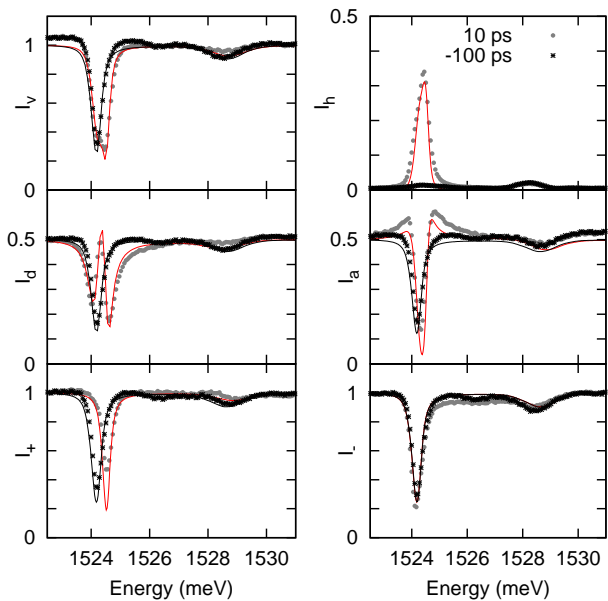


Figure 2. (Color online) Normalized reflectivity spectra detected in presence of optical pumping for different detection polarizations. The chosen spot on the sample surface corresponds to  $\Delta = -3$  meV. Pump power  $P \simeq 1$  mW. Black points correspond to the delay of 10 ps, gray points are taken at the positive delay of -100 ps. Lines show the results of fitting.

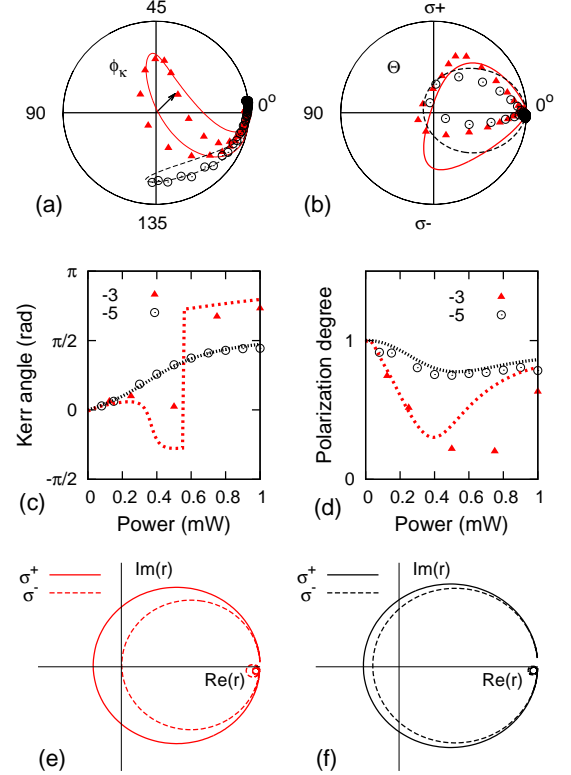
exponential is determined by spin relaxation of resident electrons, with the time constant of several nanoseconds.

With increasing pump power, the Kerr rotation amplitude becomes too large for detecting it with the optical bridge. In this case, a polarization analysis of the reflected probe spectra is necessary. Figure 2 presents examples of polarized reflection spectra in the vicinity of MC mode before and after the pump pulse for  $\Delta \simeq -3$  meV. The polarization of the reflected probe beam is seen to vary strongly, besides the variation is different for different optical frequencies. In vertical linear polarization,  $I_v$ , the MC mode splits, and a signal in orthogonal horizontal polarization,  $I_h$ , appears. In circular polarization, coinciding with that of the pump (co-circular,  $I_+$ ), a spectral shift of the MC mode is observed, which is virtually absent in the cross-circular polarization,  $I_-$ .

Figure 3(a,b) shows the hodograph of the Stokes vector under variation of the detection energy for two different detunings of the photon mode,  $\Delta \simeq -3$  and  $-5$  meV. Fig. 3(a) shows its projection on the equatorial plane. The projection on the vertical plane, containing the initial polarization of incident probe beam is shown in Fig. 3b. The Kerr rotation angle  $\phi_K$ , determined in this case as the deviation of the Stokes vector from X axis in the equatorial plane, and the ellipticity angle  $\theta$ , determined as a deviation in vertical plane, both have a complex spectral dependence. Definition of the maximum rotation angle reached in course of this evolution depends on the choice of an arbitrary integer  $m$ :  $\phi_k = 0.5(\arctan(S_2/S_1) + \pi * m)$ . This choice may be based, for instance, on the condition of continuity of the function  $\phi_k(\omega)$  (in this case, the maximum rotation angle exceeds  $\pi$ ), or on the requirement that  $\phi_k = 0$  far from the resonance both on the high- and low-frequency sides (in this case,  $\phi_K^{max} = 3/4\pi$ ). We find the latter option more reasonable. The maximum Kerr rotation angles extracted in this way are shown on Fig.3c as a function of pump power, absorbed in the sample. The hodograph of the Stokes vector for  $\Delta \simeq -5$  meV never turns around zero, and the power dependence of maximum Kerr angle is monotonic in this case [Fig. 3(c), black circles]. For  $\Delta \simeq -3$  meV it crosses zero at absorbed power of about 0.5 mW that leads to the discontinuity in power dependence [Fig.3(c), red triangles].

The appearance of a noticeable vertical component of the Stokes vector of reflected probe indicates development of ellipticity at both detunings. At some spectral points, the probe polarization becomes almost entirely circular. Moreover, considerable depolarization of the probe occurs, as indicated by the reduced length of the Stokes vector. The total polarization degree,  $p = \sqrt{S_1^2 + S_2^2 + S_3^2}$ , as a function of absorbed power is shown on Fig.3(d). It is seen that for  $\Delta \simeq -5$  meV the reflected probe always remains highly polarized, while for  $\Delta \simeq -3$  meV significant depolarization takes place.

Figure 3. (Color online) (a) Projection of the polarization of reflected probe on the equatorial plane of Poincare sphere as a function of detection energy for different detunings. Black circles:  $\Delta = -5$  meV,  $P = 0.4$  mW. Red triangles:  $\Delta = -3$  meV,  $P = 1$  mW. Lines show results of fitting. (b) The same in the vertical plane of the Poincare sphere (ellipticity angle). (c) Maximum rotation angle as a function of pump power for  $\Delta = -5$  meV and  $\Delta = -3$  meV. (d) Degree of the total polarization at the energy of maximum rotation angle for  $\Delta = -5$  meV and  $\Delta = -3$  meV. (e) Calculated function  $r(\omega)$  on the complex plane for co-(dashed line) and cross-(solid line) circular polarizations of detection for  $\Delta = -5$  meV. (f) The same for  $\Delta = -3$  meV.



The solid lines shows the results of modelling, discussed below.

The observed behaviour of polarization of the reflected probe pulse is well described in the framework of the classical model of strong-coupling microcavity. The reflection coefficient of the cavity in absence of pumping is given by the function  $r(\omega)$ , obtained by summation of waves reflected from all the heterointerfaces,

$$r(\omega) = 1 + \frac{2t_1^2}{t_1^2 + t_2^2} \frac{i\Gamma}{\omega_c - \omega - i(\Gamma + \Gamma_s) - \sum_{j=1}^3 \frac{g_j^2}{\omega_j - \omega - i\Gamma_j}} \quad (1)$$

where  $\omega$  is the incident wave frequency,  $\omega_c$  is the cavity eigenfrequency,  $\Gamma$ ,  $\Gamma_s$  are rates of radiative and non-radiative decay of photons in the microcavity,  $g_j$  is the

Transition	$\omega_j$ (meV)	$\Gamma_j$ (meV)	$g_j$ (meV)
Heavy exciton	1528.0	0.3	1.8
Light exciton	1532.0	0.3	1.4
Upper level exciton	1534	0.3	0.5

Table I. Exciton parameters for fitting of the reflection spectrum. Photon mode parameters:  $t_1 = 0.0075$ ,  $t_2 = 0.00172$ ,  $\Gamma_s = 5\mu\text{eV}$

strength of coupling between exciton and the light field,  $\omega_j$  is the exciton resonance frequency in the quantum well, in frequency units,  $\Gamma_j$  is the exciton damping. The index  $j$  denotes the type of exciton: heavy, light, or the upper level (HH2S1P) exciton.

The list of parameters, obtained by fitting the reflectivity spectra with this formula, is given in Table 1.

Fig.3(e,f) presents a trajectory of the reflection coefficient of the microcavity as a function of frequency in the complex plane. While the frequency passes the cavity resonance, the function  $r(\omega)$  makes a circle on the complex plane, starting from real unity and eventually coming back. The radius of this circle is determined by detuning  $\Delta = \omega_c - \omega_x$ . For this reason, depending on the detuning, the complex reflection coefficient may either circumvent the origin, or not. At some detuning it goes exactly through the origin, reflectivity turning to zero, which corresponds to the optical impedance matching. In our structure, the impedance matching occurs at  $\Delta = -3$  meV.

For modelling the spectral dependence of photoinduced Kerr rotation and ellipticity, we introduce two reflection coefficients,  $r^+$  and  $r^-$ , for right- and left-circular polarizations of light, respectively. These values are then used to compose a Jones matrix that is further used to calculate Stokes vector components of the reflected light for a given polarization of the incident light. When calculating the reflection spectra as functions of detuning, we took into account all the three observed resonances. In modelling Kerr signals, only heavy and light excitons were taken into account, because the upper-level exciton is far in energy and its contribution is negligible. The optical pumping was accounted for through its effect upon the parameters of heavy exciton only. This is an approximation, because creation of heavy excitons changes the oscillator strength of light excitons as well. But changing of the light-hole exciton parameters results in Kerr rotation only in the spectral vicinity of the light-hole exciton, leaving the Kerr signal on the photon mode and heavy-hole exciton virtually unaffected.

The effect of optical pumping was modelled by the linear dependence of exciton energy,  $\omega_x$ , and of the coupling constant,  $g_x$ , in the co-circular polarization on the pump power with the following parameters.

$\Delta$ , meV	$d\omega_x, *10^{-11}$ eV*cm <sup>2</sup>	$dg_x, 10^{-11}$ eV*cm <sup>2</sup>
-3	-0.6	-0.35
-5	-0.4	-0.4

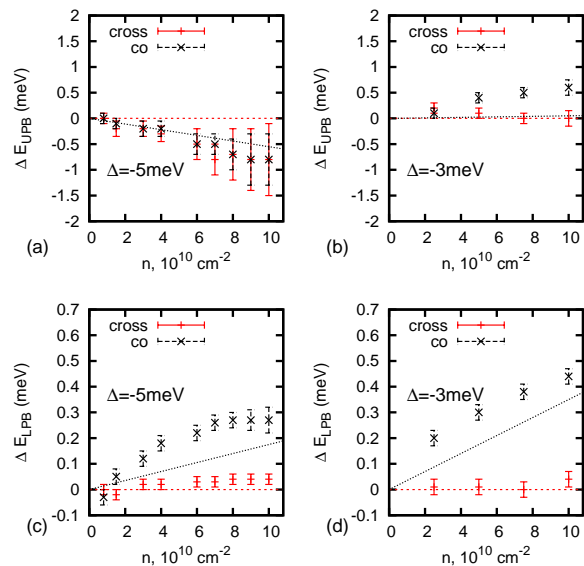


Figure 4. (Color online) Photoinduced energy shifts of the upper and lower polariton branches in co- (black crosses) and cross (red lines) circular polarization of detection. (a, c)  $\Delta = -5$  meV. (b, d)  $\Delta = -3$  meV. Lines are the corresponding energy shifts obtained by the fit.

In cross-circular polarization, the change of the spectrum under pump was assumed negligible. Linear dependence of the exciton parameters on the pump power leads to approximately linear energy shifts of the lower and upper polariton branches,  $\Delta E_{UPB}$  and  $\Delta E_{LPB}$  that, in turn, leads to the circular birefringence of the sample and the Kerr rotation. As it's seen from experimental data [see fig. 4],  $E_{LPB}$  increases at both detunings while  $E_{UPB}$  decreases at  $\Delta = -5$  meV and increases at  $\Delta = -3$  meV.

At  $\Delta = -3$  meV, as seen in Fig.3(e), showing the behavior of the reflection coefficient on the complex plane in co- and cross-polarizations, in cross-polarization the resonator remains below the impedance matching point (IMP), while in the co-polarization IMP is crossed. This is a result of reduction of the coupling constant, which diminishes absorption of co-polarized light in the cavity. Since, as mentioned above, in the first and second cases the spectral behavior of the reflection phase is considerably different, the Kerr rotation signal acquires a complex form as shown in Fig.3(a). At  $\Delta = -5$  meV the absorption in the cavity is initially weaker, so that in absence of pumping the reflection is dominated by the leakage wave. This fact explains a more simple dependence of the Kerr signal on frequency, observed in this case.

Having in mind applications of microcavity structures for all-optical modulation of light, it is desirable that the reflected light remained linearly polarized within some range of wavelengths, not only at one wavelength. This

can be realized if the reflection dip at the photon mode is small. In the idealized case when such a dip is absent, there would be no ellipticity at all wavelengths. The appearance of the dip in the reflection spectrum of a resonator with high-reflectivity back mirror is due to exciton absorption, background absorption in mirrors and lateral leakage of light. Near the exciton resonance the exciton absorption dominates over all the other losses. To keep the polarization of reflected light linear, one should change detuning in such a way as to diminish the exciton absorption, i.e. go to large negative detunings. However, this also results in a decrease of exciton contribution to the dielectric constant at the cavity mode frequency. Coupling of the exciton with the pump light also decreases. Fortunately, since the imaginary part of the dielectric function decreases as the second power of detuning, while the real part as the first power, it is possible to find an optimal detuning where absorption is still weak but the change of dielectric constant under pumping is sufficiently strong to split the photon mode. In our case, this optimal detuning is about -5 meV.

In conclusion, photoinduced KR in SC MC in the strong coupling regime can reach almost  $\pi$ . Polariton nonlinearity can be strong enough to achieve LPB shift of order of its width, for the detuning negative enough to place the cavity below impedance matching condition.

*Acknowledgements.* This work was partially supported by the Russian Ministry of Education and Science (Contract No. 11.G34.31.0067 with SPbSU). The authors acknowledge Saint-Petersburg State University for a research grant 11.38.213.2014. RVC thanks RFBR for financial support, project No. 14-02-31846.

- 
- [1] Arnold, C., Loo, V., Lemaître, A., Sagnes, I., Krebs, O., Voisin, P., Senellart, P., and Lanco, L., *Phys. Rev. X* **4**, 021004 (2014).
  - [2] Awschalom, D. D., Loss, D., and Samarth, N., eds., *Semiconductor Spintronics and Quantum Computation* (Springer, Berlin, 2002).
  - [3] Black, E. D., *American Journal of Physics* **69**, 79 (2001).
  - [4] Brunetti, A., Vladimirova, M., Scalbert, D., André, R., Solnyshkov, D., Malpuech, G., Shelykh, I. A., and Kavokin, A. V., *Phys. Rev. B* **73**, 205337 (2006).
  - [5] Cubian, D. P., Haddad, M., André, R., Frey, R., Roosen, G., Diego, J. L. A., and Flytzanis, C., *Phys. Rev. B* **67**, 045308 (2003).
  - [6] Giri, R., Cronenberger, S., Vladimirova, M., Scalbert, D., Kavokin, K. V., Glazov, M. M., Nawrocki, M., Lemaître, A., and Bloch, J., *Phys. Rev. B* **85**, 195313 (2012).
  - [7] Hu, C. Y., Young, A., O'Brien, J. L., Munro, W. J., and Rarity, J. G., *Phys. Rev. B* **78**, 085307 (2008).
  - [8] Kaliteevskii, M. A., Kavokin, A. V., and Kop'ev, P. S., *Semiconductors* **31** (1997).
  - [9] Kavokin, A. V., Vladimirova, M. R., Kaliteevski, M. A., Lyngnes, O., Berger, J. D., Gibbs, H. M., and Khitrova, G., *Phys. Rev. B* **56**, 1087 (1997).
  - [10] Lagoudakis, P. G., Martin, M. D., Baumberg, J. J., Qarry, A., Cohen, E., and Pfeiffer, L. N., *Phys. Rev. Lett.* **90**, 206401 (2003).
  - [11] Pezeshki, B., Williams, G. A., and Harris, J. S., *Applied Physics Letters* **60**, 1061 (1992).
  - [12] Poltavtsev, S. V., Ryzhov, I. I., Cherbunin, R. V., Mikhailov, A. V., Kopteva, N. E., Kozlov, G. G., Kavokin, K. V., Zapasskii, V. S., Lagoudakis, P. V., and Kavokin, A. V., *Phys. Rev. B* **89**, 205308 (2014).
  - [13] Rapaport, R., Cohen, E., Ron, A., Linder, E., and Pfeiffer, L. N., *Phys. Rev. B* **63**, 235310 (2001).
  - [14] Salis, G. and Moser, M., *Phys. Rev. B* **72**, 115325 (2005).